

# Omnidirectional absolute band gaps in two-dimensional photonic crystals

Zhi-Yuan Li and Younan Xia

Department of Chemistry, University of Washington, Box 351700, Seattle, Washington 98195

(Received 30 May 2001; published 28 September 2001)

A plane-wave expansion method has been developed to investigate the off-plane propagation of electromagnetic waves in a two-dimensional (2D) photonic crystal. Photonic band-structure calculations indicate that some 2D crystal structures can support a common band gap for both polarizations and for all off-plane angles from  $0^\circ$  up to  $90^\circ$ . The presence of such an omnidirectional absolute band gap implies that a 2D photonic crystal can exhibit some of the functionalities of a three-dimensional crystal with a complete band gap.

DOI: 10.1103/PhysRevB.64.153108

PACS number(s): 42.70.Qs, 42.25.-p, 78.20.Ci

In recent years, a significant effort has been directed towards photonic crystals—periodic dielectric materials characterized by photonic band gaps (PBG's). A PBG can prohibit the propagation of electromagnetic (EM) waves whose frequencies fall within the band gap region.<sup>1–3</sup> These materials are expected to find many applications in optoelectronics and optical communications, such as cavities, waveguides, light-emitting diodes, and most of all, all-optical integrated circuits. In principle, the full appreciation of the peculiar characteristics of a PBG should be best realized in a three-dimensional (3D) system that exhibits a complete band gap along all dimensions in space. This task has not been fully accomplished because of the difficulty in fabricating such 3D crystals with band gaps in the optical regime.<sup>4,5</sup> Therefore, it is of vast interest to realize as many functionalities of a 3D crystal as possible using lower-dimensional structures, which are much easier to fabricate. Great progress has been achieved in this regard, including 3D control of light in a 2D photonic crystal slab,<sup>6,7</sup> microlaser operation in a cavity formed in an index-guided 2D photonic crystal slab,<sup>8</sup> and omnidirectional external reflection by a 1D photonic crystal.<sup>9,10</sup>

The interest in 2D photonic crystals has been mainly concentrated on the in-plane (plane of periodicity, designated as the  $XY$  plane) propagation of EM waves. There exists a range of band gaps in various types of crystal structures. A few studies have also been dedicated to the off-plane propagation.<sup>11–15</sup> The photonic band structures thus far calculated<sup>11–13</sup> correspond to an experimental configuration where the parallel wave-vector component  $k_z$  is constant for all frequencies, even at the long-wavelength limit  $\omega=0$ . More realistic configuration should be a constant incident angle for all frequencies, and thus, different  $k_z$  for different frequencies. Although a transfer-matrix approach has been used<sup>14</sup> to calculate the transmission spectra at various incident angles, and a total reflection was found for an off-plane angle up to  $85^\circ$ , a more direct approach to view the exact position of the band gap should be the calculations of photonic band structures. In this paper, we will develop an approach for this particular task, and show the possibility for some 2D crystal structures to have an omnidirectional absolute band gap (by which we mean a common band gap for both polarizations and all off-plane incident angles from  $0^\circ$  to  $90^\circ$ ).

To achieve a common band gap, we first need a structure that exhibits an in-plane absolute band gap for both  $E$  and  $H$  polarization modes. The triangular lattice of air cylinders in a dielectric matrix is an excellent candidate.<sup>2</sup> Consider an experimental setup with a plane EM wave incident from air onto the crystal at an off-plane angle of  $\theta$ ; the eigenmode in the 2D photonic crystal has an off-plane wave-vector component  $k_z = k_0 \sin \theta$  where  $k_0 = \omega/c$ . Note that  $k_z$  is an invariant in different regions of the crystal, either the air holes or the dielectric matrix. The EM fields possess the form of a general Bloch wave:

$$\begin{aligned} \mathbf{E}(\mathbf{r}, z) &= e^{ik_0 \sin \theta z} \sum_{\mathbf{G}} \mathbf{E}_{\mathbf{G}} e^{i\mathbf{k}_{\mathbf{G}} \cdot \mathbf{r}}, \\ \mathbf{H}(\mathbf{r}, z) &= e^{ik_0 \sin \theta z} \sum_{\mathbf{G}} \mathbf{H}_{\mathbf{G}} e^{i\mathbf{k}_{\mathbf{G}} \cdot \mathbf{r}}. \end{aligned} \quad (1)$$

Here  $\mathbf{k}_{\mathbf{G}} = \mathbf{k} + \mathbf{G}$ , with  $\mathbf{k}$  and  $\mathbf{G}$  being the Bloch wave vector and reciprocal vectors in the 2D lattice plane.

The EM fields satisfy Maxwell's equations,

$$\nabla \times \mathbf{E} = ik_0 \mathbf{H}, \quad \nabla \times \mathbf{H} = -ik_0 \epsilon(\mathbf{r}) \mathbf{E}. \quad (2)$$

If we directly substitute Eq. (1) into the standard wave equation for pure magnetic or pure electric fields, as has been done in previous calculations,<sup>2,11–13,16–19</sup> we will have a highly complex eigenproblem, because every matrix element involves the eigenvalue  $k_0$ . To overcome this difficulty, we consider the in-plane components of both electric and magnetic fields. From Eq. (2), we have

$$\begin{aligned} \frac{\partial}{\partial z} E_x &= \frac{1}{-ik_0} \frac{\partial}{\partial x} \left[ \frac{1}{\epsilon} \left( \frac{\partial}{\partial x} H_y - \frac{\partial}{\partial y} H_x \right) \right] + ik_0 H_y, \\ \frac{\partial}{\partial z} E_y &= \frac{1}{-ik_0} \frac{\partial}{\partial y} \left[ \frac{1}{\epsilon} \left( \frac{\partial}{\partial x} H_y - \frac{\partial}{\partial y} H_x \right) \right] - ik_0 H_x, \\ \frac{\partial}{\partial z} H_x &= \frac{1}{ik_0} \frac{\partial}{\partial x} \left( \frac{\partial}{\partial x} E_y - \frac{\partial}{\partial y} E_x \right) - ik_0 \epsilon E_y, \\ \frac{\partial}{\partial z} H_y &= \frac{1}{ik_0} \frac{\partial}{\partial y} \left( \frac{\partial}{\partial x} E_y - \frac{\partial}{\partial y} E_x \right) + ik_0 \epsilon E_x. \end{aligned} \quad (3)$$

In Fourier space, we have

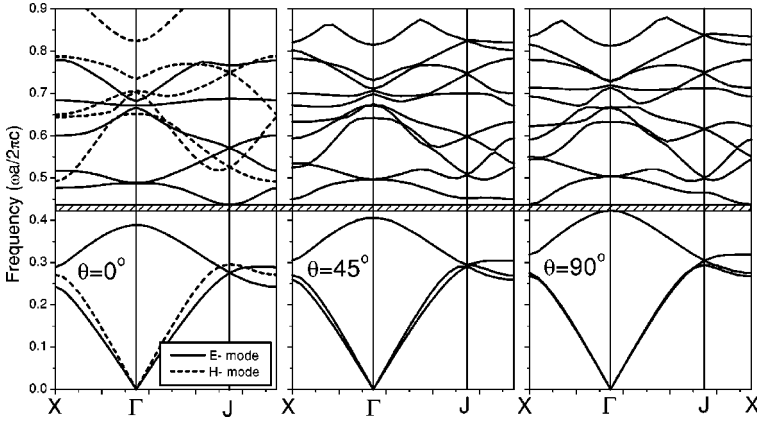


FIG. 1. Plots of photonic band structures for a triangular lattice of air cylinders embedded in a dielectric matrix at different off-plane incidence angles of EM waves:  $0^\circ$  (left panel),  $45^\circ$  (middle panel), and  $90^\circ$  (right panel). A common band gap is represented by the cross-hatched region. The crystal has a filling fraction of air cylinders  $f=0.75$ , and a refractive index  $n=3.6$  for the dielectric.

$$\begin{aligned}
 k_0^2 \sin \theta E_G^x &= -k_G^x \sum_{G'} \epsilon_{G,G'}^{-1} (k_G^x H_{G'}^y - k_{G'}^y H_G^x) + k_0^2 H_G^y, \\
 k_0^2 \sin \theta E_G^y &= -k_G^y \sum_{G'} \epsilon_{G,G'}^{-1} (k_G^x H_{G'}^y - k_{G'}^y H_G^x) - k_0^2 H_G^x, \\
 k_0^2 \sin \theta H_G^x &= k_G^x (k_G^x E_G^y - k_G^y E_G^x) - k_0^2 \sum_{G'} \epsilon_{G,G'} E_{G'}^y, \\
 k_0^2 \sin \theta H_G^y &= k_G^y (k_G^x E_G^y - k_G^y E_G^x) + k_0^2 \sum_{G'} \epsilon_{G,G'} E_{G'}^x. \quad (4)
 \end{aligned}$$

Here  $\epsilon_{G,G'}$  is the Fourier coefficient of  $\epsilon(\mathbf{r})$ .

Equation (4) is a standard eigenproblem formulation, albeit it involves the time-consuming diagonalization of a  $(4N) \times (4N)$  matrix ( $N$  being the number of plane waves used). We found that it could be simplified into a  $(2N) \times (2N)$  eigenproblem by making transformations

$$h_{G,1} = k_G^x E_G^y - k_G^y E_G^x, \quad h_{G,2} = k_G^x H_G^y - k_G^y H_G^x. \quad (5)$$

After some analytical derivations, Eq. (4) can be reduced to

$$\begin{pmatrix} T_{11} & T_{12} \\ T_{21} & T_{22} \end{pmatrix} \begin{pmatrix} h_1 \\ h_2 \end{pmatrix} = k_0^2 \begin{pmatrix} h_1 \\ h_2 \end{pmatrix}. \quad (6)$$

Here  $h_1$  ( $h_2$ ) denotes a column matrix composed of  $\{h_{G,1}\}$  ( $\{h_{G,2}\}$ ), and the matrices  $T_{ij}$  are defined as  $T_{11}^{G,G'} = -P_0^{G,G'}(\mathbf{k}_G \cdot \mathbf{k}_{G'})$ ,  $T_{21}^{G,G'} = \sin \theta P_0^{G,G'}(k_G^x k_{G'}^y - k_G^y k_{G'}^x)$ ,  $T_{12}^{G,G'} = -\sin \theta [k_G^x (P_0 Y_2)_{G,G'} - k_G^y (P_0 Y_1)_{G,G'}]$ , and  $T_{22}^{G,G'} = -k_G^x [(\sin^2 \theta P_0 - I) Y_1]_{G,G'} - k_G^y [(\sin^2 \theta P_0 - I) Y_2]_{G,G'}$ , where  $I$  is an unit matrix,  $Y_1^{G,G'} = k_G^x \epsilon_{G,G'}^{-1}$ ,  $Y_2^{G,G'} = k_G^y \epsilon_{G,G'}^{-1}$ , and  $P_0 = (\sin^2 \theta I - \epsilon_{G,G'})^{-1}$ . When  $\theta=0$ , Eq. (6) can be decoupled to the standard eigenproblem for the  $E$  ( $h_2$ ) and  $H$  ( $h_1$ ) polarization modes of in-plane propagation.<sup>2,18,19</sup> At  $\theta>0$ , these two modes are coupled to each other.

With a greatly simplified eigenproblem in hand, we can now go ahead to calculate the photonic band structures for a 2D crystal under an arbitrary incident angle  $\theta$ . Figure 1 displays the results for a triangular lattice of air cylinders in a dielectric matrix with a refractive index of  $n=3.6$ . The air

cylinder has a filling fraction of  $f=0.75$ , and a radius of  $r=0.455a$ , where  $a$  is the lattice constant. The left panel of Fig. 1 shows the results for the in-plane propagation ( $\theta=0$ ) for both  $E$  (solid lines) and  $H$  (dashed lines) polarization modes. The overlap of the  $E$  2-3 band gap and the far wider  $H$  1-2 band gap creates an absolute band gap, with the band edges lying at the  $\Gamma$  and  $J$  symmetry points, respectively. The absolute band gap lies at frequency  $0.389 - 0.437(2\pi c/a)$ , with a normalized size (ratio of gap width to midgap frequency) of 11.6%. Here  $c$  is the light speed in vacuum. At an off-plane angle of  $\theta=45^\circ$ , both the upper and lower band edges shift towards higher frequencies of  $0.406$  and  $0.450(2\pi c/a)$ , respectively. When  $\theta$  continues to increase and reaches  $90^\circ$ , the lower band edge moves upwards continuously to a frequency of  $0.423(2\pi c/a)$ , while the upper band edge downshifts to a frequency of  $0.438(2\pi c/a)$ . In spite of the shift of these band edges, especially at the  $\Gamma$  point, we still obtain a residual common band gap for all off-plane angles up to  $90^\circ$ . This omnidirectional absolute band gap (shown in Fig. 1 by the crosshatched region) lies between  $0.423 - 0.437(2\pi c/a)$ , with its normalized size (3.2%) greatly reduced relative to the in-plane gap.

The opening of an omnidirectional absolute band gap can be more clearly seen from Fig. 2, where the dependence of the band-edge positions on the off-plane angle are plotted for two different filling fractions ( $f=0.75$  and  $0.8$ ) and for crystal structures with a refractive index contrast of  $3.6$  and  $4.0$ , respectively. Denoted by the horizontal solid ( $f=0.75$ ) and dotted ( $f=0.8$ ) lines, the common band gap is found to be determined by two extreme situations with  $\theta=0$  and  $90^\circ$ . When  $\theta$  is increased from  $0$ , the lower band edge moves monotonously towards higher frequencies, while the upper band edge first shifts upwards, and arrives at a maximum value somewhere, then moves downwards. For the crystal with  $f=0.8$  and  $n=3.6$ , we find a common gap at  $0.454 - 0.467(2\pi c/a)$  with a normalized size of 2.8%, a little bit smaller than that for  $f=0.75$ . At a larger refractive index contrast as  $n=4.0$  (which is the refractive index of germanium in the infrared regime), the common band gap becomes far wider, opening at  $0.377 - 0.401(2\pi c/a)$  and  $0.405 - 0.445(2\pi c/a)$  for  $f=0.75$  and  $0.8$ , with the corresponding gap size being 6.2% and 9.4%, respectively. For this system a larger size of air cylinders is more competent to widen the common band gap.

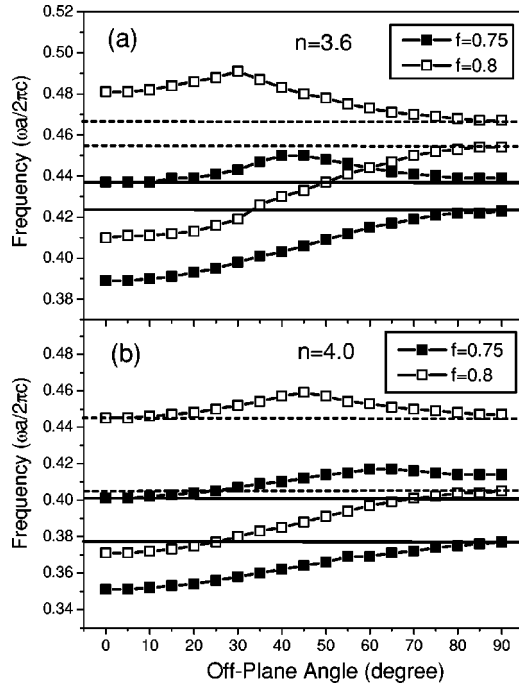


FIG. 2. Dependence of the band edges on the off-plane angle for  $f=0.75$  and  $0.8$  in a triangular lattice of air cylinders in dielectric. The refractive index contrast is (a)  $n=3.6$  and (b)  $n=4.0$ . The common band gap is indicated by the horizontal solid ( $f=0.75$ ) and dashed ( $f=0.8$ ) lines.

We next investigate the dependence of the common band gap on the refractive index contrast of the above triangular lattices. The results are displayed in Fig. 3 for a filling fraction of  $0.75$  and  $0.8$ . The size of the common band gap in both structures increases monotonously with respect to the refractive index contrast. The opening of this gap imposes a stringent limit on the refractive index contrast: It must be as strong as  $3.4$ . Figure 3 also indicates that a smaller  $f$  is more competent for opening the common gap when the refractive index contrast is below  $3.7$ . It should also be noted that when  $f$  is reduced to  $0.7$ , the common gap disappears even at a refractive index as high as  $n=3.6$ . Therefore, the presence of an omnidirectional absolute band gap can only be accomplished in a 2D crystal with a sufficiently large refractive index contrast and filling fraction.

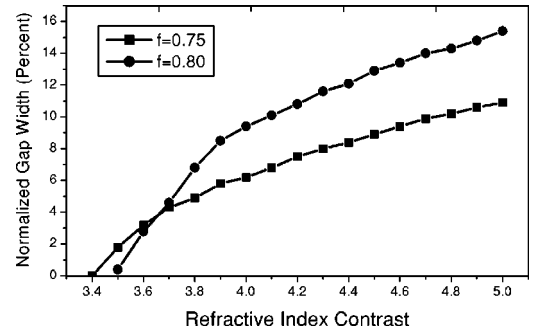


FIG. 3. Dependence of the common band-gap size on the refractive index contrast in a triangular lattice of air cylinders in dielectric at  $f=0.75$  and  $0.8$ .

We finally consider a different type of crystal structure, a triangular lattice of anisotropic dielectric cylinders in air. It has been shown<sup>18</sup> that such a crystal structure with the cylinders made of a positive uniaxial material can open an absolute band gap for the in-plane propagation. It is interesting to see whether this band gap can survive in the off-plane propagation. The material we study here is tellurium (Te), a uniaxial solid with extraordinarily large refractive indices and a very strong positive anisotropy in the infrared regimes (the ordinary and extraordinary refractive indices are  $n_o=4.8$ , and  $n_e=6.2$ , respectively). In our calculations, the extraordinary axis is set to be parallel to the longitudinal axis of the cylinders ( $z$  axis), so we have principal refractive indices as  $n_z=n_e=6.2$ ,  $n_x=n_y=n_o=4.8$ . This structure has been shown<sup>18</sup> to exhibit a large in-plane absolute band gap for both  $E$  and  $H$  polarization modes. The band structures are calculated using the standard plane-wave expansion method<sup>17-19</sup> and displayed in the left panel of Fig. 4 for  $f=0.4$ . The off-plane band structures (shown in the middle and right panels of Fig. 4) are calculated using an approach similar to that derived for isotropic crystal structures [see Eqs. (1)–(6)], with only some slight modifications.

For the in-plane propagation, we find an overlap between the  $H$  1-2 and  $E$  4-5 band gaps, with the former completely covered by the latter, leaving an absolute band gap between  $0.232-0.280(2\pi c/a)$ , and with a normalized size of  $18.8\%$ . When the EM wave propagates in a direction out of the plane, we expect that the band edges of the absolute band gap should shift and lead to a reduced size of the common

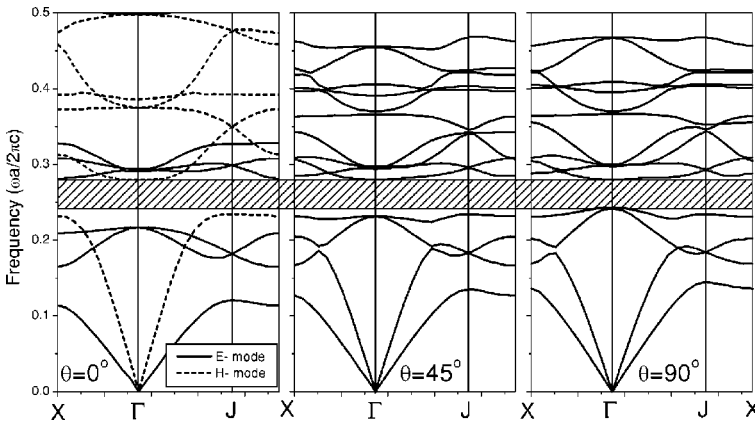


FIG. 4. Plots of photonic band structures for a triangular lattice of tellurium cylinders in air at different off-plane incidence angles of EM waves:  $0^\circ$  (left panel),  $45^\circ$  (middle panel), and  $90^\circ$  (right panel). A common band gap is represented by the cross-hatched region. The tellurium cylinder has a filling fraction of  $f=0.4$ , and the extraordinary axis is parallel to the longitudinal axis of the cylinders.

gap. One significant feature found in this crystal is a far-smaller reduction in the common gap for an off-plane angle up to  $90^\circ$ , as compared to the case of dielectric cylinders in air shown in Figs. 1 and 2. The common band gap is represented in Fig. 4 by the cross-hatched region, and lies between  $0.242 - 0.280(2\pi c/a)$  with a size of 14.6%. The reason for this modest reduction is that the in-plane band gap is determined by the  $H$  1 band (the lower band edge), which is well above the  $E$  3 band. Therefore, there is some space of off-plane angle for the  $E$  3 band to first evolve to exceed the  $H$  1 band, before it finally serves as the lower band edge and determines the size of the common gap. If the common band gap is measured by the  $\Gamma$  point of the  $E$  3 band, like in Fig. 1, an over 40% size reduction of the common gap is found compared to the in-plane gap, while the real size reduction is about 20%.

Now we have seen that there can exist omnidirectional absolute band gaps in some 2D photonic crystal structures. Although these are not true 3D complete band gaps (as is clear when we observe that the band gap in Figs. 1–4 will be closed for an infinitely large  $k_z$  well beyond  $k_z = k_0 \sin 90^\circ = k_0$ ), they can still find a lot of applications, such as omnidirectional reflectors, mirrors, microcavities, and photonic crystal fibers.<sup>20</sup> More importantly, these omnidirectional absolute band gaps offer a potential to model the functionalities of 3D photonic crystals with low-dimensional structures that are easier to fabricate. Since any EM wave with  $k_z$  up to  $k_0$  (or a propagation angle in air up to  $90^\circ$ ) is inhibited in our structures, and a large part of these 2D crystal structures is occupied by air, we expect light emit-

ted from a source embedded in the air region will be largely confined three dimensionally around the source, provided that the light source has a configuration such that the emitted light has negligible components of large off-plane wave momentum with  $k_z > k_0$ . This can be achieved when the light source has a size along the  $z$  axis larger than the wavelength of the emitted light. It is interesting to make a comparison with the recently discussed<sup>9,10</sup> 1D photonic crystals that can function as omnidirectional reflectors for external incident light. These 1D structures only support an off-plane band gap for those  $k_z$  below  $k_0$ , while all composite materials are of a refractive index larger than 1. Therefore, all homogeneous wave components with  $k_z$  between  $k_0$  and  $nk_0$  ( $n$  being the lowest refractive index in the crystal) will leak out of the crystal, and thus the 3D confinement cannot be achieved.

In summary, we have developed a plane-wave expansion method to account for the dependence of band gaps in a 2D photonic crystal on the off-plane incident angle of EM waves. Omnidirectional absolute band gaps were found in some 2D crystal structures. These simple 2D structures may allow one to realize some of the functionalities of a 3D photonic crystal. For example, incorporation of such 2D structures into an ordinary photonic crystal plane slab may significantly improve the efficiency of microlasers.<sup>8</sup>

The authors gratefully acknowledge the financial support in part from the David and Lucile Packard Foundation, the Alfred P. Sloan Foundation, the Dreyfus Foundation, and the Washington Technology Center.

<sup>1</sup>E. Yablonovitch, Phys. Rev. Lett. **58**, 2059 (1987).

<sup>2</sup>J.D. Joannopoulos, R.D. Meade, and J.N. Winn, *Photonic Crystals* (Princeton University Press, Princeton, NJ, 1995).

<sup>3</sup>Z.Y. Li, L.L. Lin, and Z.Q. Zhang, Phys. Rev. Lett. **84**, 4341 (2000).

<sup>4</sup>S.Y. Lin, J.G. Fleming, D.L. Hetherington, B.K. Smith, R. Biawas, K.M. Ho, M.M. Sigalas, W. Zubrzycki, S.R. Kurtz, and J. Bur, Nature (London) **394**, 251 (1998).

<sup>5</sup>S. Noda, K. Tomoda, N. Yamamoto, and A. Chutinan, Science **289**, 604 (2000).

<sup>6</sup>S.G. Johnson, S. Fan, P.R. Villeneuve, J.D. Joannopoulos, and L.A. Kolodziejski, Phys. Rev. B **60**, 5751 (1999).

<sup>7</sup>E. Chow, S.Y. Lin, S.G. Johnson, P.R. Villeneuve, J.D. Joannopoulos, J.R. Wendt, G.A. Vawter, W. Zubrzycki, H. Hou, and A. Alleman, Nature (London) **407**, 983 (2000).

<sup>8</sup>O. Painter, R.K. Lee, A. Scherer, A. Yariv, J.D. O'Brien, P.D. Dapkus, and I. Kim, Science **284**, 1819 (1999).

<sup>9</sup>J.N. Winn, Y. Fink, S. Fan, and J.D. Joannopoulos, Opt. Lett. **20**, 1573 (1998).

<sup>10</sup>Y. Fink, J.N. Winn, S. Fan, C. Chen, J. Michel, J.D.

Joannopoulos, and E.L. Thomas, Science **282**, 1679 (1998).

<sup>11</sup>A.A. Maradudin and A.R. McGurn, J. Mod. Opt. **41**, 275 (1994).

<sup>12</sup>J.N. Winn, R.D. Meade, and J.D. Joannopoulos, J. Mod. Opt. **41**, 257 (1994).

<sup>13</sup>X.P. Feng and Y. Arakawa, IEEE J. Quantum Electron. **32**, 535 (1996).

<sup>14</sup>M.M. Sigalas, R. Biawas, K.M. Ho, and C.M. Soukoulis, Phys. Rev. B **58**, 6791 (1998).

<sup>15</sup>S. Foteinopoulou, A. Rosenberg, M.M. Sigalas, and C.M. Soukoulis, J. Appl. Phys. **89**, 824 (2001).

<sup>16</sup>K.M. Ho, C.T. Chan, and C.M. Soukoulis, Phys. Rev. Lett. **65**, 3152 (1990).

<sup>17</sup>Z.Y. Li, J. Wang, and B.Y. Gu, Phys. Rev. B **58**, 3721 (1998).

<sup>18</sup>Z.Y. Li, B.Y. Gu, and G.Z. Yang, Phys. Rev. Lett. **81**, 2574 (1998); Eur. Phys. J. B **11**, 65 (1999).

<sup>19</sup>D. Cassagne, C. Jouanin, and D. Bertho, Phys. Rev. B **53**, 7134 (1996).

<sup>20</sup>J.C. Knight, J. Broeng, T.A. Birks, and P.St. J. Russell, Science **282**, 1476 (1998).